Influence of FTDP-17 mutants on circTau RNAs

Giorgi Margvelani[1*], Justin R. Welden[2*], Andrea Arizaca[1], Sandra Sardon[1] and Stefan Stamm[1, +]

[1]Department of Molecular and Cellular Biochemistry, University of Kentucky, Lexington, KY, USA
[1, 2]Sanders-Brown Center on Aging, University of Kentucky, Lexington, KY, USA

* joint first authors

+ corresponding author: stefan@stamms-lab.net

Abstract
At least 53 mutations in the microtubule associated protein tau gene (MAPT) have been identified that cause frontotemporal dementia. 47 of these mutations are localized between exons 7 and 13. They could thus affect the formation of circular RNAs (circRNAs) from the MAPT gene that occur through backsplicing from exon 12 to either exon 10 or exon 7. Five FTDP-17 mutations increase the formation of 12->7 circRNA and three different mutations increase the amount of 12->10 circRNA. CircRNAs are translated after undergoing adenosine to inosine RNA editing, catalyzed by ADAR enzymes. We found that the interferon induced ADAR1-p150 isoform has the strongest effect on circTau RNA translation. ADAR1-p150 activity had a stronger effect on circTau RNA expression and strongly decreased 12->7 circRNA and unexpectedly increased 12->10 circRNA. In both cases, translation of tau circRNAs was strongly promoted. Unexpectedly, we found that the 12->7 circTau protein interacts with eucaryotic initiation factor 4B (eIF4B), which is reduced by four FTDP-17 mutations located in the second microtubule domain. These are the first studies of the effect of human mutations on circular RNA formation and translation. They show that point mutations influence circRNA expression levels, likely through changes in the secondary pre-mRNA structures. The effect of the mutations is voided by editing of the circular RNAs, leading to their translation. Thus circular RNAs and their editing status should be considered when analyzing FTDP-17 mutations.

Introduction

CircTau RNAs

Circular RNAs (circRNAs) are a recently identified class of RNAs, generated through backsplicing of a 5′ splice site to a downstream 3′ splice site[1]. They are expressed in many tissues at low levels, usually less than 1% of their linear counterparts[2, 3]. CircRNAs are highly expressed in brain[4-7], cytosolic and enriched in synaptosomes. Changes in expression of 33 circRNAs have been detected in parietal cortex in AD[8]. When combined with publicly available datasets, 14 circRNAs were associated with Braak stages and explained 31% of the clinical dementia rating, compared to 5% of the APOE4 alleles[8].

CircRNAs were found to be translated[9-11] from reporter constructs, which was surprising, as circRNAs lack ribosomal entry sites or a 5′ cap to allow translational initiation. We found that adenosine to inosine (A>I) RNA editing strongly promotes translation of circRNAs[12, 13], suggesting that inosines could provide a ribosomal entry site. CircRNAs are more stable than linear mRNAs, with a half-life of 2-4 days[14, 15], which compares to an average half-life of 4 hrs for mRNAs[16]. Due to intramolecular base pairing, circRNAs form rod like structures with extended double strand RNA sequences[17], and are thus more prone to undergo modifications by ADAR enzymes (adenine deaminase acting on RNA) that recognize double stranded RNA structures and convert adenosines into inosines[18]. Humans express three ADAR enzymes: ADAR1 expressed in all tissues with an interferon-induced cytosolic (p150) and a constitutive nuclear (p110) isoform; ADAR2 showing weak expression in brain and the catalytic inactive ADAR3 showing strong expression in brain.

FTDP-17 mutations cause tauopathies

The human microtubule-associated protein tau (MAPT) stabilizes microtubules in the brain[19] through up to four microtubule binding repeats, formed by exons 7-12. Exon 10 encodes the second microtubule-binding repeat and is alternatively spliced in adult human brain that contains a mixture of tau proteins with 3 or 4 microtubule binding repeats[20], which is changed in disease[21-23], especially in several forms of frontotemporal dementia with parkinsonism linked to chromosome 17 (FTDP-17), now called frontotemporal lobar degeneration (FTLD-TAU)[24]. In Alzheimer's disease and related tauopathies, tau protein mis-folds into intracellular, insoluble protein polymers[25] and intraneuronal tau inclusions (neurofibrillary tangles, or NFTs) that are the pathological feature most strongly associated with cognitive status.

We found that the tau gene generates two circular RNAs[26] that are translated after A>I RNA editing[12]. The circtau proteins promote the aggregation of linear tau protein *in vitro* and in reporter cells[12]. Circtau RNAs are divisible by three and do not contain a stop codon. They thus form multimers of the tau microtubule repeat regions.

At least 53 mutations in the *MAPT* gene cause familial tauopathies have been identified. 38/53 of these mutations are in the circtau RNAs and 9/53 of them are in the introns surrounding exon 10[24]. Thus 47/53 of all FTLD-TAU mutations could influence properties of circular RNAs. Two FTDP-17 mutations, V337M and K317M strongly increase translation of the start-codon-less tau 12->10 circRNA, suggesting that some FTDP-17 mutations could act through circtau RNAs[12].

Here we analyze the influence of exonic FTDP-17 mutants on circTau RNA and circTau protein formation and expression. We found that distinct FTDP-17 mutants increase circTau protein and circTau RNA expression levels. All circTau RNAs with FTDP-17 mutants were expressed as proteins after undergoing A>I editing. There is no correlation between the circRNA amounts and levels of generated proteins, suggesting a predominant translational regulation for the formation of circTau proteins. Unexpectedly, we found that the 12->7 circTau protein binds to eukaryotic initiation factor 4B (eIF4B), which is reduced by FTDP-17 mutants located in the second microtubule binding domain in exon 10, suggesting a new mode of action for some FTDP-17 mutants.

Material and Methods

Transfection

We performed transfection in Human Embryonic Kidney (HEK) 293T cells. 4µg aliquots of Plasmid DNA were mixed with sterile 150mM 150µl NaCl, in a ratio of 1µg DNA per 3 µl polyethyleneimine solution (1µg/µl), (PEI; Polysciences, 24765-1), co transfection were at 1:1 (4µg:4µg), for total RNA (1µg:1µg). The mixture was incubated at room temperature for 25 min and added to cells, cultured in 150mm dish (Alkali scientific TDN0150) for protein experiment and in 6-well culture plate (VWR, 100062-892) for total RNA experiment and transfected at around 50-60% confluency. Cells were lysed and analyzed after 96h of transfection.

Isolation of circTau protein

For the extraction of circtau protein we used M2 anti-Flag magnetic beads at ration 10µl per 1mg. Protein were eluted using 15µg anti-Flag peptide, for the other experiment we boiled the beads in Sodium Dodecyl sulfate (SDS) running buffer.
We generate tau fibrils by mixing 4µg of purified tau protein with 1µg of linear 2N4R tau WT protein in the pretense of 500ng yeast t-RNA and incubated for 72h.

Antibodies and Western Blot

Cells were lysed in non SDS low RIPA buffer (150mM NaCl, 50mM tris pH 7,4, 1% NP-40) and boiled for 5 min in 95°C, protein concentration were determined by Molecular Probes Quanti iT Qubit Protein Assay kit (Fisher Scientific Q33211) and tau-Flag Lysates pre cleaned with Mouse IgG Coupled 4% agarose beads (Aviva Systems Biology, OOIB00007) and Benzonase (EDM Millipore 71205-3). Similar number of aliquots were applied to the gel and SDS gel electrophoresis and Western Blot carried out as described previously (one of the supplementary). Nitrocellulose membranes were stained with Ponceau S solution to confirm uniform transfer of proteins. Membranes were stained using commercially available antibodies: Magnetic Beads Anti-FLAG, Mouse Monoclonal Antibody M2 (1:1000) (Sigma-Aldrich M8823) and Anti 4R-tau Antibody (1:1000) (Cosmo Bio CAC-TIP-4RT-P01). For the loading control - Anti-Calreticulin antibody ER marker [EPR3924] (Abcam ab92516), like tau protein, calreticulin is also heat stable.

Protein aggregation and Transmission electron microscopy

After 72h incubation in vitro tau fibrils sonicated for 10 min in a water bath, before the preparation of sample for TEM, grids were exposed to UV light for 1h. 5µl aliquot of sonicated fibril samples loaded onto a carbon-coated, 300 mesh copper grid (Electron

Microscopy Sciences, CF300-CU-50) and allowed to be absorbed for 5 min. Negative staining was performed by 3µl 2% Uranyl Acetate, applied per grid and incubated for 2 min. After that, excess stain was wicked off and grid was washed twice with a 5µl deionized water and air-dried. Imaging carried on using FEI Talos F200X TEM (ThermoFisher Scientific) at University of Kentucky Electron Microscopy Center.

Expression constructs

The DNA constructs were generated using Gibson cloning New England Biolabs [27], and the final constructs were deposited into Addgene, with accession numbers (203365 - 203368, 203371 -203376, 203378, 203379, 203382 - 203388, 203390, 203391).

RT-PCR and taqman probes

The TaqMan assays were performed using a one-step TaqMan probe kit (TaqMan™ RNA-to C_T™ *1-Step* Kit, Invitrogen), using the primer set. As the TaqMan probe we used 12->7 Probe FAM– ACCATCAGCCCCCTTTTTATTTCCT-MGBNFQ. For GAPDH loading control, the GAPDH TaqMan Probe, Invitrogen, Hs02786624_g1 was used. Primers used were Tau Junction 12->7 set2 F – TCGAAGATTGGGTCCCTGGA and Tau Junction 12->7 set2 R - TTTTGCTGGAATCCTGGTGG

TnT reaction and pull-down

The TnT Quick Coupled Transcription/Translation System (Promega) was used to generate 35S-labeled eIF4B. The circ tau 12-7 WT protein was isolated as described through immunoprecipitation from cellular extracts using 10ul of M2 anti-Flag magnetic beads per 1mg of total protein [12]. The beads were resuspended in 1X TBST buffer and mixed with 20 µl of resuspended beads with 5 µl of each TNT product and brought up to 35 µl with 1X TBST. The samples were incubated at 4 ºC overnight with agitation, followed by 3 times washing with 50 µl 1X TBST in 100 µM NaCl. Samples were analyzed on PAGE gels and imaged using a Typhoon FLA 9500.

Results

<u>FTDP-17 mutations influence expression levels the 12->7 circTau proteins</u>

To test the effect of FTDP-17 mutants on circTau protein expression, we used circTau expression constructs that we transfected into HEK293 cells. The wild-type construct lacking FTDP-17 mutants has been described previously [12]. It consists of exons 7-13 without the internal introns and is flanked 1384 and 957nt of the natural introns six and thirteen. We introduced selected FTDP17-mutations into this construct and determined protein expression using a 3xFLAG tag in exon 7 (**Fig. 1A**). Similar to linear tau protein, circTau proteins are heat stable and as described we used the supernatant of boiled lysates for analysis [12].

We previously reported that circular RNAs are translated after undergoing adenosine to inosine RNA editing, caused by ADAR1 or ADAR2 [12, 28]. There are two major isoforms of ADAR1: ADAR1-p150 and ADAR1-p110. They differ in the N-terminal Z-dsRNA binding domain and a nuclear export signal, which are present only in ADAR1-p150 [29]. The two domains are included due to an upstream promoter that is induced by interferon-alpha. We thus first compared ADAR1-p150 and ADAR1-p110 for their ability

to induce circTau RNA translation by cotransfecting GFP, ADAR1-p110 and ADAR1-p150 expression constructs with circTau wild-type expression constructs into HEK293 cells. The presence of ADAR1 activity strongly increased protein abundance and ADAR1-p150 had an about 5-fold stronger effect than ADAR1-p110, even though western blot analysis showed that in the transfection experiments ADAR2 was expressed slightly higher than ADAR2 (**Fig. 1B**). For further experiments, we thus concentrated on the ADAR1-p150 isoform.

The effect of FTDP-17 mutations on circTau protein formation was next tested in cotransfection experiments using expression clones for ADAR1-p150 and the various FTDP-17 mutants. To avoid problems with possible uneven immunoprecipitations due to the FTDP-17 mutations, we exploited the heat stability of circTau-proteins and analyzed boiled lysates of the transfected cells. The amount of FLAG-tagged circTau proteins was compared with endogenous calreticulin, a protein that is also heat stable [30]. The 12->7 circTau RNA lacks a stop codon and most likely a stretch of four inosines causes termination of the rolling circle translation. Similar to wild-type, the major translation product of circTau proteins harboring the FTDP-17 mutations is 38 kDa that was seen for all mutants. When compared to wild-type, two mutants, S305N and V363I showed a statistically significant higher protein expression. Our data indicate that two FTDP-17 mutations impact protein expression levels of circTau proteins.

<u>FTDP-17 mutations influence expression of non-edited circTau 12->7 RNA that is reduced by ADAR1-p150</u>

To date, not much is known about translation of circular RNAs. To start getting insights into the translational mechanism of circTau RNAs, we first ask whether there is a correlation between the amounts of circTau RNA and the corresponding protein. We devised a taqman assay using a custom-made taqman probe flanked by PCR-primers in the circRNA (**Fig. 2A**). The taqman probe was used with 1 µg of total RNA in a one step reverse-transcriptase reaction. We first used total RNA from cells cotransfected with 12->7 expression constructs cotransfected with GFP. Since taqman assays for circular RNAs are novel, we further validated the PCR products after 40 cycles on agarose gels and observed the predicted 216 nt band for all mutants tested (**Supplemental Figure 2A, B**). CircTau RNA was determined from total RNA by calculating the delta ct values of circTau RNA and linear GAPDH. Notably, our assay is sensitive enough to omit the RNase R digestion step used in most circRNA isolation procedures and generated only one band. When using RNAseR treated total RNA that is enriched for circular RNAs, we observed multiple bands due to rolling circle reverse transcription (**Supplemental Figure 2C),** which could complicate a taqman assay.

The 12->7 circTau RNA was normalized to GAPDH mRNA. In contrast to protein expression, several FTDP17-mutants, mainly G303V, K317M and V337M strongly increased circTau RNA expression (**Fig. 2B**).

Unlike the protein, circTau RNA is generated in the absence of ADAR1, allowing us to compare the circTau RNA expression levels in the absence and presence of ADAR1 activity. We thus repeated the experiment using total RNA from cells transfected with 12->7 circTau expression constructs and ADAR1-p150.

With the exception of K257T, ADAR1-p150 presence reduced circTau RNA expression levels. When combined all mutants are combined, ADAR1-p150 causes an

about three-fold reduction in RNA expression (**Fig. 2B, right**). Thus, some FTDP-17 mutants influence the expression of non-edited circTau RNA. This effect is antagonized by RNA-editing caused by ADAR1-p150 that generally reduces circTau12->7 RNA expression.

FTDP-17 mutations influence expression levels of the 12->10 circTau proteins

The MAPT gene generates two major circRNAs through backsplicing from exon12 to either exon 7 or exon 10. We thus next tested selected mutations in the 12->10 circTau RNA background, using the expression construct shown in **Figure 3A**. In contrast to the 12->7 circTau RNA, the 12->10 circTau RNA lacks a start codon, which can be introduced by RNA editing where an AUA codon is changed to an AUI codon that can initiate translation [12, 31]. In addition, the V337M and K317M FTDP-17 mutations introduce start codons and promote translation in the absence of cotransfected ADAR-activity [12] (**Fig 3B**).

We first compared ADAR1-p150 and ADAR1-p100 for their ability to promote circTau RNA translation, using the wild-type, the K317 and V337M mutations. As we previously reported, in the absence of ADAR-activity there is hardly any protein expression detectable from the wild-type, likely due to the absence of a start codon. However, ADAR-activity strongly promoted circTau protein expression. Similar to the 12->7 circRNAs, ADAR1-p150 has a much stronger effect than ADAR1-p110 (**Figure 3B**). In the absence of cotransfected ADAR activity, the K317M and V337M mutations result in weak protein formation, which is strongly increased by ADAR1. As shown in Figure 3B, ADAR-p150 promotes the translation of the start codon-less 12->10 circRNA stronger than the introduction of a start codon.

We next tested selected mutants for their influence on 12->10 circTau protein formation by cotransfecting their expression clones with ADAR1-p150 expression clones in HEK293 cells. All mutants resulted in a protein with the same size as the wild type. Similar to the 12->7 tau circRNA, we quantified the expressed 12->10 circTau proteins by comparing them to calreticulin in boiled lysates. As in the 12->7 background, the mutants N296N and K369I had a significant higher expression than wild-type (**Figure 2D**). V363I had a higher expression in the 12->10 background, but no effect on the 12->7 circTau RNA. Conversely, P301S and S305I increased expression from the 12->7 background but had no effect on the 10->12 background. We conclude that two mutants, N296N, and K369I have a similar enhancing effect on circTau protein expression, but in general the effect of FTDP-17 mutations on protein expression depends on their location in a 12->7 or 12->10 circular RNA background.

ADAR1-p150 increases expression levels of the 12->10 circTau RNA

To gain further insight into the translational mechanism of circTau RNAs, we measured the RNA levels of selected FTDP-17 mutations in the 12->10 background. Several designs of taqman probes did not work and we thus performed qPCR using SYBR green (**Fig. 4A**) with the primers indicated in **Supplementary Figure 3.** Similar to the qPCR analysis of the 12->7 circTau RNA, we used total RNA from transfected cells and omitted the RNase R treatment step. As shown in **Supplemental Figure 4**, the qPCR resulted in only one band, making the detection with SYBR green possible. The signal from circTau RNA was normalized to linear GAPDH mRNA, measured in a taqman assay.

In the absence of ADAR1 activity, the FTDP-17 mutations S305I, V363I and K369I strongly increased 12->10 circTau RNA expression. Upon cotransfection of ADAR1-p150, we observed strong expression of five mutants: P301S, G303V, S305N, S305I, and V363I (**Fig. 4B**). The change in 12->10 circRNA levels is not reflected on the protein level that showed uniform expression (**Fig. 3**), indicating that 12->10 circTau protein formation is mainly regulated on the translational level. Thus, ADAR1-p150 has different effects on circRNA expression, depending on the circRNA sequence and possibly flanking introns.

Effect of ADAR1-p150, ADAR2 and ADAR3 on translation of FTDP-17 mutants.

FTDP-17 mutations vary in age of onset [32] and their effect on the assembly of tau into filaments [33]. Likewise, ADAR-enzymes are not uniformly expressed throughout the brain. ADAR1 and ADAR2 are expressed in neurons, but not astrocytes throughout the brain. ADAR1 expression is lowest in cortex, choroid plexus and hippocampus, whereas ADAR2 shows lowest expression in cortex and hippocampus and high expression in thalamus [34]. The catalytic inactive variant ADAR3 is expressed only in brain. We thus asked whether FTDP-17 mutants respond differently to ADAR-1, -2 and -3 and tested eight mutants.

The same amounts of expression clones for these mutants were cotransfected with ADAR expression clones and protein expression in boiled lysates was normalized to calreticulin found in the lysates and quantified. For all mutants tested, ADAR1-p150 had a stronger effect than ADAR2 (**Figure 5**). However, compared to all other mutants, ADAR2 has a weaker effect on P301S. For most mutants, we saw a slight increase of protein with the catalytic inactive variant ADAR3 when compared to the GFP control, that reached/not reached statistical significance. Similar results were observed, when we analyzed the transfection data with an anti-tau antiserum (**Supplemental Figure 2**). The slight increase of circTau protein due to ADAR3 was surprising, but we previously observed it using wild-type constructs and also found slight changes in circTau RNA editing [12]. We speculate that ADAR3 transfection increases ADAR1 or ADAR2 activity due to an autoregulatory effect. The data show that ADAR1-p150 had the strongest effect on translation of circTau RNAs harboring FTDP-17 mutants, but there there are slight mutant-specific variations caused by ADAR2 and ADAR3.

Proteins made from the 12->7 circTau RNA interact with eucaryotic initiation factor 4B

When validating the circTau proteins through mass-spectrometry, we detected interacting proteins in the immunoprecipitates that were generated from previously boiled lysates (**Supplemental Figure 6**). Other than tau, eukaryotic initiation factor 4B (eIF4B) was the most abundant interacting protein. This finding was unexpected, as binding from eIF4B to the linear tau protein has not been reported.

We first confirmed the specific interaction between 12->7 circTau protein and endogenous eIF4B in immunoprecipitation experiments. To directly test a possible binding to linear tau protein, we expressed a linear 3xFLAG-N04R construct[12], as well as the 12->7 and 12->10 tau circRNA expression constructs in HEK293 cells. All proteins were immunoprecipitated from heat-treated lysates using FLAG antibodies. We first confirmed the expression of the expected proteins by testing the immunoprecipitates with anti-FLAG. Using the same volumes of cell lysates, we found that linear 3xFLAG-N04R protein is expressed about 10-fold stronger than the circular proteins (**Fig. 6A, left**). Next,

we tested the immunoprecipitates with an anti-eIF4B antibody, which showed presence of eIF4B in the immunoprecipitates of the circular 12->7 circRNA encoded protein (**Figure 6A, right**), validating the interaction we observed in mass-spectrometry. The interaction with the 12->10 circRNA encoded protein was significantly weaker. Importantly, we could not detect and interaction between linear tau protein and eIF4B (**Fig. 6A, right**), even though the linear tau protein was expressed much higher. The data suggest that eIF4B interacts predominately with the protein products of the 12->7 circtau RNAs. The 12->7 circTau protein is highly similar to a fragment of the linear 3xFLAG-N04R protein and differs only in the exon junction region. Thus, the lack of interaction between eIF4B and 3xFLAG-N04R thus suggests a highly specific interaction between the 12->7 circtau encoded protein and eIF4B.

EIF4B consists of several domains involved in interactions with various proteins (**Fig. 6B**). The N-terminal domain binds to poly A binding protein [35], the RNA recognition motif and an arginine-rich domain that binds to RNA [36], the C-terminal that binds to eIF4A [37]and the DRYG repeat domain binds to eIF3A and aids in eIF4B dimerization [38].

Given the propensity of eIF4B's domains to interact with different proteins, we hypothesized that similarly eIF4B interacts with 12->7 circTau protein using a specific domain. To determine this interaction site, we expressed ^{35}S-labled eIF4B variants in reticulate lysates and incubated 12->7 circTau wild-type protein bound to agarose through the FLAG tag. We analyzed flow-throughs and bound protein, which were visualized using the radioactive label. We observed eIF4B lacking the DYRG domain in the flowthrough, but in the interaction matrix. All other constructs containing a DYRG domain showed binding to the 12->7 circTau-protein resin (**Fig. 6B, right**). These findings indicate that the DYRG domain mediates the interaction between eIF4B and circTau proteins.

FTLD-17 mutations located in exon 10 reduce the interaction between eIF4B and 12->7 circTau protein.

We next tested the interaction between FTLD-mutants in the 12->7 circTau background and eIF4B. The mutant 12->7 circTau proteins were overexpressed in HEK293 cells and immunoprecipitated from heat treated lysates using anti-Flag. The FLAG-tagged 12->7 circTau protein and endogenous eIF4B were detected in the immunoprecipitates. We then normalized the signal of eIF4B to the 12->7 circTau signal seen in the immunoprecipitates. We saw a reduction of eIF4B binding in the mutants P301S, G303V, S305N and S305I, located in exon 10 (**Fig. 6C, D**). Our immunoprecipitation experiments (**Fig. 6A**) indicate that eIF4B binds much weaker to the 12->10 circTau protein. We next tested the influence of selected mutations in the 12->10 circTau background and compared to wild-type observed a reduction for eIF4B binding for G303V and P301L, two FTDP-17 mutations located in exon 10 (**Supplemental Figure 7**). All mutations affecting eIF4B binding are located in the second microtubule binding domain in exon 10 suggesting that this region of the circTau protein participates in binding to eIF4B.

Discussion

The human MAPT-gene generates circular RNAs [26] that are translated [12] after some of their adenosine residues are enzymatically converted into inosines in A>I RNA editing. As 47/53 FTDP-17 mutations are located in regions that could contribute to

circTau RNA generation, we studied for the first time the effect of FTDP-17 mutations on circTau RNA formation and translation.

Circular RNAs can be analyzed by Taqman probes.

Not much is known about the editing-dependent translation of circRNAs and we thus first set up a Taqman assay to quantify circRNA expression levels. In general, the primer options for circRNAs are limited and in the circTau case design programs do not find optimal Taqman sequences. We thus made Taqman probes against the unique backsplice junction and initially followed the rules for linear RNAs, i.e. a length of 16-30 nt, the melting points about 10-15 ºC higher than the PCR primers and a GC-content of 30-80% and found that the successful taqman probe worked with a melting temperature of 5 ºC higher than the amplification primers. In our design we avoided a run of G-nucleotides present in the sense strand by using the reverse complement. We omitted the RNase R digestion step, as it resulted in multiple bands, probably as a result of priming with RNA fragments and/or rolling circle reverse transcription that is known to generate a 'ladder' of PCR amplicons from circular RNAs [39]. Our 12->7 circTau taqman assay generates only one amplicon and thus allows to measure 12->7 circTau RNA.

ADAR1-p150 has the strongest effect on circRNA translation

Using RNAseq, we previously measured RNA editing of circTau RNAs in HEK293 cells and found very low editing levels in the absence of cotransfected ADAR activity, that are most likely due to the endogenous ADAR1 present in HEK293 cells [12]. For all FTDP-17 mutants tested, translation of the circTau RNAs is strongly promoted by ADAR activity, provided in our experimental system by cotransfection with ADAR1 or ADAR2 expression clones. The ADAR1 protein is present in two isoforms. Similar to ADAR2, the constitutive ADAR1-p110 isoform is predominantly localized in the nucleus. In contrast, the interferon-induced ADAR1-p150 isoform is predominantly cytosolic[18, 40] as in addition to the N-terminal Z-alpha domain it contains a nuclear export sequence. The Z-alpha domain is a dsRNA binding domain that binds to Z-RNAs [41]. It remains to be determined whether circRNAs predominantly adopt the Z-RNA conformation making them preferred substrates for ADAR1-p150. As ADAR1-p150 is induced by interferons, the translation of circRNAs could be a direct consequence of released interleukins and thus relevant for Alzheimer's diseases that is characterized by inflammation [42-44].

No correlation between circRNA and circProtein expression levels

We expressed circTau RNAs in HEK293 cells by transfecting expression constructs harboring FTDP-17 mutants and measured both circTau protein and circTau RNA expression levels. We observed differences in circTau RNA expression levels for some FTDP-17 mutants. Since all circTau expression constructs were driven by the same promoter in an identical background, the changes are unlikely to be due to a transcriptional effect. A more probable explanation is that mutants interfere with circRNA formation by changing the pre-mRNA structure. ADAR1-p150 coexpression strongly decreases 12->7 circTau expression, and strongly promotes 12->7 circTau translation. Some FTDP-17 mutants cause differences in edited 12->7 circTau RNA expression that are not reflected on the protein level, suggesting that circRNA translation is mainly regulated through factors independent from circRNA substrate abundance, such as

translational initiation. Thus, any analysis of the pathophysiological role of FTDP-17 mutants should not only rely on circRNA levels.

Interaction with eIF4B

We unexpectedly found that the 12->7 circTau protein binds to eIF4B through the DYRG domain of eIF4B. This interaction is specific for the 12->7 circTau protein as it was not seen for linear N04R tau and was much weaker for the 12->10 circ proteins. eIF4B binding is a unique property of the 12->7 circTau protein, which remains to be further functionally characterized.

FTDP-17 mutation influence formation and translation of circular Tau RNAs

Our data suggest a complex interplay of FTDP-17 mutations with the formation and translation of circTau RNAs (**Figure 7**). The MAPT-pre mRNA adopts a secondary structure that promotes circRNA formation, likely by bringing backsplice sites into close proximity. The formation of a secondary pre-mRNA structure is promoted by repeat elements, in primates often Alu elements. CircRNAs form extended intermolecular base pairs and a appear as rod-like structures [17]. This base pairing generates double-stranded RNA regions that make circRNA substrates for ADAR-enzymes and multiple adenines of circTau RNAs are edited to inosines in the presence of ADAR activity. The editing efficiency for a given adenine residue is less than 10%, i.e. lower than for known edited mRNAs [12]. It is possible that FTDP-17 mutations change the circRNA structure, which could promote backsplicing, which could explain our observed increase of circTau RNA formation for five FTDP-17 mutants. ADAR-activity is known to interfere with pre-mRNA secondary structures. In humans, the major target of ADAR are Alu-elements [45], which could interfere with the pairing of the backsplice sites. We found unexpectedly that this effect is sequence-context dependent, as ADAR1 reduced 12->7 circTau RNA formation but increased 12->10 circTau RNA formation. circTau RNAs are translated after being edited and the inosines most likely aid in ribosomal entry. All FTDP-17 mutants tested are translated into protein in the presence of ADAR1 and only two mutants, S350N and V363I slightly increase this effect. When ADAR variants are compared, ADAR1-p150 had by far the strongest effect on circRNA translation, independent of the FTDP-17 mutant present. This finding could have pathophysiological significance, as ADAR1-p150 is induced by cytokines that are elevated in AD [43, 44]. Finally, we found that the 12->7 circTau protein binds to eIF4B, which is a feature distinct from linear tau protein. FTDP-17 mutations located in the second microtubule repeat binding domain reduce this interaction and could thus interfere with its function in translational initiation that needs to be determined.
Collectively, our data suggest that circular Tau RNAs should be considered, when determining the pathophysiological effect of FTDP-17 mutations.

Acknowledgments
This work was supported by the department of Defense and the National Institutes of Health.

Figures

Figure 1: FTDP-17 mutations change expression levels of proteins encoded by the 12->7 circRNA

A. Location of selected FTDP-17 mutations in the MAPT gene.

Boxes are exons, lines are introns. The arrows on top indicate the 12->10 and 12->7 backsplicing. The FTDP-17 mutations are indicated. The yellow box in exon 9 is the 3x Flag tag used for detection. The structure of the reporter gene is shown schematically underneath and was described in [12], M: single start codon in exon 9. The structure of the circular RNA and its translation product are shown on the right. IIII: stretch of inosines that could serve as a stop signal. R1-R4: microtubule repeat binding domains.

B. Effect of ADAR1-p150 and ADAR1-p110 on circTau-protein expression.

The circTau 12->7 reporter gene shown in (A) was cotransfected with expression clones for GFP, ADAR1-p150 and ADAR1-p110. CircTau protein was immunoprecipitated using anti-FLAG antisera and detected with anti-FLAG. The expression of EGFP-tagged ADAR-p150 and ADAR-p110 was tested in total cell lysates using Western Blot. Similar volumes of cell lysates were analyzed by western blot using the GFP-tag of the transfected proteins. A star indicates an unspecific band.

C. Effect of FTDP-17 mutants on circTau protein expression.

FTDP-17 mutations were introduced into the 12->7 circRNA expression construct and were cotransfected with ADAR1-p150. 4 µg expression construct was cotransfected with 4 µg ADAR1-p150 expression construct in 150 mm dishes. Lysates of the transfected cells were separated on PAGE gradient gels and analyzed by Western blot. First, we used an anti-FLAG antibody and the same membrane was reprobed with anti-calreticulin (dotted box).

D. Quantification of the protein expression.

The ratio of calreticulin signal to FLAG-tag signal was calculated and normalized to wild-type. The data represent at least three independent transfection experiments.

Figure 2: Effect of FTDP-17 mutations and ADAR1-p150 on expression of the 12->7 circTau RNA.

A. Sequence and location of the taqman probe spanning exons 12 and 7. Star: FAM, circle : MGBNFQ quencher. The location of the primers in the circRNA is schematically shown on right.

B. Quantification of at least three independent experiments. The 12->7 circTau signal was normalized to GAPDH. All date were normalized to wild-type, which was set to 1. The graph on the right shows the combined delta delta Ct values in the absence or presence of ADAR1-p150.

Figure 3: Influence of FTDP-17 mutations on expression levels of proteins encoded by the 12->10 circRNA

A. Schematic overview of the mutations in the 12->10 circTau RNA. The structure of the expression construct is schematically shown below. The circular RNA is shown on the right. The start codons introduced by the K317M and V337M mutations are indicated. The AUA>AUI editing event generates a start codon that was confirmed by mutagenesis [12]. R2-R3 are tau microtubule binding repeats.

B. Wild type, K317M and V337M expression constructs were cotransfected with GFP, ADAR1-p110 and ADAR1-p150 expression constructs. circTau protein was isolated using FLAG-immunoprecipitation and detected by FLAG.
C. Expression constructs for the indicated mutants were cotransfected with ADAR1-p150 expression constructs in HEK293 cells. Lysates were analyzed by Western blot using FLAG and calreticulin antibodies. The calreticulin exposure time is 1/10 of the FLAG-tag exposure time.
D. Quantification of the FLAG to calreticulin signal. The ratio was set to 1 for the wild-type. At least three independent transfections were analyzed.

Figure 4: Effect of FTDP-17 mutations and ADAR1-p150 on expression of the 12->10 circTau RNA.
A. Location of the primers for SYBR green assay in the 12->10 circTau RNA.
B. The endpoint PCR products were separated in a 2% agarose gel.
C. Quantification of the 12->10 circTau RNA expression of FTDP-17 mutants, which were compared to GAPDH and compared to wild-type, set to 1.

Figure 5: Response of selected FTDP-17 mutants on ADAR1-p150, ADAR2 and ADAR3.
A. Effect of ADAR1-p150, ADAR2 and ADAR3 on FTDP-17 mutants. Expression clones of the FTDP-17 mutants in the 12->7 circTau RNA background were cotransfected with expression clones for equal amounts of EGFP, ADAR1-p150, ADAR2 and ADAR3. Equal volumes of boiled lysates were analyzed by Western blot and the blots were re-tested with anti-calreticulin (dotted boxes).
B. Quantification of three independent experiments. The ratio of calreticulin to circTau-protein of three independent experiments was calculated and normalized to wild-type.

Figure 6: circTau 12->7 protein binds to eIF4B
A. Immunoprecipitation of endogenous eIF4B and linear N04R tau and circTau proteins. Clones expressing linear tau N04R, as well as 12->7 circTau and 12->10 circTau clones were transfected into HEK293 cells and immunoprecipitated with anti-FLAG. The immunoprecipitates were tested with anti-FLAG and anti-eIF4B. The lane for FLAG-N04R tau is shown with short exposure on the right. "-" empty lane to account for the strong linear tau signal.
B. Mapping of eIF4B interaction domain. The domain structure for eIF4B is shown on the left. circTau 12->7 protein was bound to agarose and incubated with eIF4B deletion variants made in reticulate lysates. Bound proteins (top) and flow-through (bottom) were analyzed by PAGE, using the radioactive ^{35}S label for detection.
C. Interaction of eIF4B and 12->7 circTau proteins. The FTDP-17 12->7 circTau mutants indicated were expressed in HEK293 cells and immunoprecipitated with anti-FLAG. The immunoprecipitates were first analyzed with anti-FLAG for circTau proteins and the with eIF4B for endogenous eIF4B binding.
D. Quantification of the eIF4B – circTau protein interaction from three independent experiments. The ratio of eIF4B/circTau protein signal was determined and normalized to wild-type.

Figure 7: Model: FTDP-17 mutations influence circTau RNA processing and translation

A. Aided by Alu-elements (arrows), the MAPT pre-mRNAs adopt secondary structures that promote circRNA formation likely by bringing backsplice sites into close proximity.
B. Several FTDP-17 mutations promote circRNA formation, possibly by changing the secondary structure.
C. RNA editing influences circRNA processing depending on the sequence context. In the 12->7 background, RNA editing reduces circRNA formation, for the 12->10 background RNA editing increases circRNA formation. FTDP-17 mutations modulate the effect of RNA editing on circRNA formation.
D. RNA editing strongly promotes circTau RNA translation and some FTDP-17 mutations further enhance circRNA translation.
E. The 12->7 circTau protein binds to eukaryotic initiation factor 4B, eIF4B, an interaction that could not be detected with linear tau protein.

Supplemental Figures

Supplemental Figure 1

The sequence of the 12->7 circTau RNA is shown. The location of the taqman probe, and the forward and reverse primers are indicated. FTDP-17 mutations are indicated on top of the sequence and the corresponding nucleotide changes are shown below.

Supplemental Figure 2

A. Gel electrophoresis of the end points of the taqman RT-PCR reactions. 12->7 expression constructs co-transfected with GFP were used. The ct values are shown on top of the gels. The expected band is 216 nt. The mutants are indicated. The top row shows detection of the circTau RNA, the bottom row shows the detections of GAPDH.
B. The experiments were similar to (A), but RNAs from HEK293 cells cotransfected with ADAR1-p150 were used.
C. Agarose gel of the RT-PCR results for circTau RNA after 40 cycles. The expected size is 315 nt and the second weaker band around 500 nt likely represents a rolling circle reverse transcription. Primers used were circdetect Fw2: AATAAGAAGCTGGATCTTAGC and circdetect rev2: GATCTTTATAATCACCGTCAT

Supplemental Figure 3

The sequence of the 12->7 circTau RNA is shown. The location of the taqman probe, and the forward and reverse primers are indicated. FTDP-17 mutations are indicated on top of the sequence and the corresponding nucleotide changes are shown below.

Supplemental Figure 4

A. Gel electrophoresis of the end points of the SYBR green reaction RT-PCR reactions. 12->10 expression constructs co-transfected with GFP were used. The ct values are shown on top of the gels. The expected band is 2 nt. The mutants are indicated. The top row shows detection of the circTau RNA, the bottom row shows the detections of GAPDH using a taqman assay.

B. The experiments were similar to (A), but RNAs from HEK293 cells cotransfected with ADAR1-p150 were used.
C. Agarose gel of the RT-PCR results for circTau RNA after 40 cycles. The expected size is 246 nt and the second weaker band of about 400 nt likely represents a rolling circle reverse transcription.

Supplemental Figure 5
Expression clones of the FTDP-17 mutants in the 12->7 circTau RNA background were cotransfected with equal amounts of expression clones for EGFP, ADAR1-p150, ADAR2 and ADAR3 and Immunoprecipitated using anti-flag. The immunoprecipitates were analyzed by Western blot using anti-flag and anti Tau antisera. The analysis of the lysates with anti-FLAG is shown in Figure 5.

Supplemental Figure 6
Proteins interaction with circTau. 12->10 and 12->7 circTau expression clones were transfected into HEK293 cells and immunoprecipitates analyzed using mass-spectroscopy after the total immunoprecipitate was digested.

Supplemental Figure 7
A. The 12->10 circTau mutants indicated were expressed in HEK293 cells and immunoprecipitated with anti-FLAG. Protein was detected in Western Blot using anti-FLAG. The immunoprecipitates were probed with eIF4B antibody for endogenous eIF4B binding.
B. Quantification of at least three independent experiments.

References

1. Yang L, Wilusz JE, Chen LL. Biogenesis and Regulatory Roles of Circular RNAs. Annu Rev Cell Dev Biol. 2022;38:263-89. Epub 20220524. doi: 10.1146/annurev-cellbio-120420-125117. PubMed PMID: 35609906.
2. Salzman J. Circular RNA Expression: Its Potential Regulation and Function. Trends Genet. 2016;32(5):309-16. Epub 2016/04/07. doi: 10.1016/j.tig.2016.03.002. PubMed PMID: 27050930; PMCID: PMC4948998.
3. Hsiao KY, Sun HS, Tsai SJ. Circular RNA - New member of noncoding RNA with novel functions. Experimental biology and medicine (Maywood, NJ). 2017;242(11):1136-41. Epub 2017/05/10. doi: 10.1177/1535370217708978. PubMed PMID: 28485684; PMCID: PMC5478007.
4. Akhter R. Circular RNA and Alzheimer's Disease. Adv Exp Med Biol. 2018;1087:239-43. Epub 2018/09/28. doi: 10.1007/978-981-13-1426-1_19. PubMed PMID: 30259371.
5. Meng S, Zhou H, Feng Z, Xu Z, Tang Y, Wu M. Epigenetics in Neurodevelopment: Emerging Role of Circular RNA. Front Cell Neurosci. 2019;13:327. Epub 2019/08/06. doi: 10.3389/fncel.2019.00327. PubMed PMID: 31379511; PMCID: PMC6658887.
6. Mehta SL, Dempsey RJ, Vemuganti R. Role of circular RNAs in brain development and CNS diseases. Prog Neurobiol. 2020;186:101746. Epub 2020/01/14. doi: 10.1016/j.pneurobio.2020.101746. PubMed PMID: 31931031; PMCID: PMC7024016.
7. Hanan M, Soreq H, Kadener S. CircRNAs in the brain. RNA Biol. 2017;14(8):1028-34. Epub 2016/11/29. doi: 10.1080/15476286.2016.1255398. PubMed PMID: 27892769; PMCID: PMC5680707.
8. Dube U, Del-Aguila JL, Li Z, Budde JP, Jiang S, Hsu S, Ibanez L, Fernandez MV, Farias F, Norton J, Gentsch J, Wang F, Dominantly Inherited Alzheimer N, Salloway S, Masters CL, Lee JH, Graff-Radford NR, Chhatwal JP, Bateman RJ, Morris JC, Karch CM, Harari O, Cruchaga C. An atlas of cortical circular RNA expression in Alzheimer disease brains demonstrates clinical and pathological associations. Nature neuroscience. 2019;22(11):1903-12. Epub 2019/10/09. doi: 10.1038/s41593-019-0501-5. PubMed PMID: 31591557; PMCID: PMC6858549.
9. Costello A, Lao NT, Barron N, Clynes M. Continuous translation of circularized mRNA improves recombinant protein titer. Metab Eng. 2019;52:284-92. doi: 10.1016/j.ymben.2019.01.002. PubMed PMID: 30615942.
10. Pamudurti NR, Bartok O, Jens M, Ashwal-Fluss R, Stottmeister C, Ruhe L, Hanan M, Wyler E, Perez-Hernandez D, Ramberger E, Shenzis S, Samson M, Dittmar G, Landthaler M, Chekulaeva M, Rajewsky N, Kadener S. Translation of CircRNAs. Mol Cell. 2017;66(1):9-21 e7. doi: 10.1016/j.molcel.2017.02.021. PubMed PMID: 28344080; PMCID: PMC5387669.
11. Abe N, Matsumoto K, Nishihara M, Nakano Y, Shibata A, Maruyama H, Shuto S, Matsuda A, Yoshida M, Ito Y, Abe H. Rolling Circle Translation of Circular RNA in Living Human Cells. Sci Rep. 2015;5:16435. doi: 10.1038/srep16435. PubMed PMID: 26553571; PMCID: PMC4639774.

12. Welden JR, Margvelani G, Arizaca Maquera KA, Gudlavalleti B, Miranda Sardón SC, Campos A, Robil N, Lee DC, Gonzalo Hernandez A, Wang W, Di J, de la Grange P, Nelson PT, Stamm S. RNA editing of microtubule associated protein tau circular RNAs promotes their translation and tau tangle formation. Nucleic Acids Res. 2022;50(22):12979-96. PubMed PMID: 36533443.
13. Arizaca Maquera KA, Welden JR, Margvelani G, Miranda Sardón SC, Hart S, Robil N, Gonzalo Hernandez A, de la Grange P, Nelson PT, Stamm S. Alzheimer's disease pathogenetic progression is associated with changes in regulated retained introns and editing of circular RNAs. Front Mol Neurosci. 2023;in press.
14. Wang C, Liu H. Factors influencing degradation kinetics of mRNAs and half-lives of microRNAs, circRNAs, lncRNAs in blood in vitro using quantitative PCR. Sci Rep. 2022;12(1):7259. Epub 20220504. doi: 10.1038/s41598-022-11339-w. PubMed PMID: 35508612; PMCID: PMC9068688.
15. Jeck WR, Sorrentino JA, Wang K, Slevin MK, Burd CE, Liu J, Marzluff WF, Sharpless NE. Circular RNAs are abundant, conserved, and associated with ALU repeats. Rna. 2013;19(2):141-57. Epub 2012/12/20. doi: 10.1261/rna.035667.112. PubMed PMID: 23249747; PMCID: 3543092.
16. Herzog VA, Reichholf B, Neumann T, Rescheneder P, Bhat P, Burkard TR, Wlotzka W, von Haeseler A, Zuber J, Ameres SL. Thiol-linked alkylation of RNA to assess expression dynamics. Nat Methods. 2017. doi: 10.1038/nmeth.4435. PubMed PMID: 28945705.
17. Sanger HL, Klotz G, Riesner D, Gross HJ, Kleinschmidt AK. Viroids are single-stranded covalently closed circular RNA molecules existing as highly base-paired rod-like structures. Proc Natl Acad Sci U S A. 1976;73(11):3852-6. PubMed PMID: 1069269; PMCID: PMC431239.
18. Samuel CE. Adenosine deaminase acting on RNA (ADAR1), a suppressor of double-stranded RNA-triggered innate immune responses. J Biol Chem. 2019;294(5):1710-20. doi: 10.1074/jbc.TM118.004166. PubMed PMID: 30710018; PMCID: PMC6364763.
19. Wang Y, Mandelkow E. Tau in physiology and pathology. Nat Rev Neurosci. 2016;17(1):5-21. doi: 10.1038/nrn.2015.1. PubMed PMID: 26631930.
20. Andreadis A. Tau gene alternative splicing: expression patterns, regulation and modulation of function in normal brain and neurodegenerative diseases. Biochem Biophys Acta. 2005;1739:91-103.
21. Ishizawa K, Ksiezak-Reding H, Davies P, Delacourte A, Tiseo P, Yen SH, Dickson DW. A double-labeling immunohistochemical study of tau exon 10 in Alzheimer's disease, progressive supranuclear palsy and Pick's disease. Acta Neuropathol. 2000;100(3):235-44. doi: 10.1007/s004019900177. PubMed PMID: 10965792.
22. Glatz DC, Rujescu D, Tang Y, Berendt FJ, Hartmann AM, Faltraco F, Rosenberg C, Hulette C, Jellinger K, Hampel H, Riederer P, Moller HJ, Andreadis A, Henkel K, Stamm S. The alternative splicing of tau exon 10 and its regulatory proteins CLK2 and TRA2-BETA1 changes in sporadic Alzheimer's disease. J Neurochem. 2006;96:635-44. PubMed PMID: 16371011.
23. Qian W, Liang H, Shi J, Jin N, Grundke-Iqbal I, Iqbal K, Gong CX, Liu F. Regulation of the alternative splicing of tau exon 10 by SC35 and Dyrk1A. Nucleic

Acids Res. 2011;39(14):6161-71. Epub 20110405. doi: 10.1093/nar/gkr195. PubMed PMID: 21470964; PMCID: PMC3152345.
24. Ghetti B, Oblak AL, Boeve BF, Johnson KA, Dickerson BC, Goedert M. Invited review: Frontotemporal dementia caused by microtubule-associated protein tau gene (MAPT) mutations: a chameleon for neuropathology and neuroimaging. Neuropathol Appl Neurobiol. 2015;41(1):24-46. doi: 10.1111/nan.12213. PubMed PMID: 25556536; PMCID: PMC4329416.
25. Lee VM, Goedert M, Trojanowski JQ. Neurodegenerative tauopathies. Annu Rev Neurosci. 2001;24:1121-59. doi: 10.1146/annurev.neuro.24.1.1121. PubMed PMID: 11520930.
26. Welden JR, van Doorn J, Nelson PT, Stamm S. The human MAPT locus generates circular RNAs. Biochim Biophys Acta Mol Basis Dis. 2018:2753-60. doi: 10.1016/j.bbadis.2018.04.023. PubMed PMID: 29729314.
27. Gibson DG, Young L, Chuang RY, Venter JC, Hutchison CA, 3rd, Smith HO. Enzymatic assembly of DNA molecules up to several hundred kilobases. Nat Methods. 2009;6(5):343-5. doi: 10.1038/nmeth.1318. PubMed PMID: 19363495.
28. Arizaca Maquera KA, Welden JR, Margvelani G, Miranda Sardón SC, Hart S, Robil N, Hernandez AG, de la Grange P, Nelson PT, Stamm S. Alzheimer's disease pathogenetic progression is associated with changes in regulated retained introns and editing of circular RNAs. Frontiers in Molecular Neuroscience. 2023;16. doi: 10.3389/fnmol.2023.1141079.
29. Song B, Shiromoto Y, Minakuchi M, Nishikura K. The role of RNA editing enzyme ADAR1 in human disease. Wiley Interdiscip Rev RNA. 2022;13(1):e1665. Epub 20210608. doi: 10.1002/wrna.1665. PubMed PMID: 34105255; PMCID: PMC8651834.
30. Wijeyesakere SJ, Gafni AA, Raghavan M. Calreticulin is a thermostable protein with distinct structural responses to different divalent cation environments. J Biol Chem. 2011;286(11):8771-85. Epub 20101222. doi: 10.1074/jbc.M110.169193. PubMed PMID: 21177861; PMCID: PMC3058961.
31. Licht K, Hartl M, Amman F, Anrather D, Janisiw MP, Jantsch MF. Inosine induces context-dependent recoding and translational stalling. Nucleic Acids Res. 2019;47(1):3-14. doi: 10.1093/nar/gky1163. PubMed PMID: 30462291; PMCID: PMC6326813.
32. Boeve BF, Hutton M. Refining frontotemporal dementia with parkinsonism linked to chromosome 17: introducing FTDP-17 (MAPT) and FTDP-17 (PGRN). Arch Neurol. 2008;65(4):460-4. doi: 10.1001/archneur.65.4.460. PubMed PMID: 18413467; PMCID: PMC2746630.
33. Goedert M, Ghetti B, Spillantini MG. Frontotemporal dementia: implications for understanding Alzheimer disease. Cold Spring Harb Perspect Med. 2012;2(2):a006254. doi: 10.1101/cshperspect.a006254. PubMed PMID: 22355793; PMCID: PMC3281593.
34. Jacobs MM, Fogg RL, Emeson RB, Stanwood GD. ADAR1 and ADAR2 expression and editing activity during forebrain development. Dev Neurosci. 2009;31(3):223-37. Epub 20090327. doi: 10.1159/000210185. PubMed PMID: 19325227; PMCID: PMC2692045.

35. Bushell M, Wood W, Carpenter G, Pain VM, Morley SJ, Clemens MJ. Disruption of the interaction of mammalian protein synthesis eukaryotic initiation factor 4B with the poly(A)-binding protein by caspase- and viral protease-mediated cleavages. J Biol Chem. 2001;276(26):23922-8. Epub 20010323. doi: 10.1074/jbc.M100384200. PubMed PMID: 11274152.
36. Methot N, Pause A, Hershey JW, Sonenberg N. The translation initiation factor eIF-4B contains an RNA-binding region that is distinct and independent from its ribonucleoprotein consensus sequence. Mol Cell Biol. 1994;14(4):2307-16. doi: 10.1128/mcb.14.4.2307-2316.1994. PubMed PMID: 8139536; PMCID: PMC358597.
37. Rozovsky N, Butterworth AC, Moore MJ. Interactions between eIF4AI and its accessory factors eIF4B and eIF4H. RNA. 2008;14(10):2136-48. Epub 20080821. doi: 10.1261/rna.1049608. PubMed PMID: 18719248; PMCID: PMC2553726.
38. Methot N, Song MS, Sonenberg N. A region rich in aspartic acid, arginine, tyrosine, and glycine (DRYG) mediates eukaryotic initiation factor 4B (eIF4B) self-association and interaction with eIF3. Mol Cell Biol. 1996;16(10):5328-34. doi: 10.1128/MCB.16.10.5328. PubMed PMID: 8816444; PMCID: PMC231531.
39. Boss M, Arenz C. A Fast and Easy Method for Specific Detection of Circular RNA by Rolling-Circle Amplification. Chembiochem. 2020;21(6):793-6. Epub 20191127. doi: 10.1002/cbic.201900514. PubMed PMID: 31584239; PMCID: PMC7154740.
40. George CX, Samuel CE. STAT2-dependent induction of RNA adenosine deaminase ADAR1 by type I interferon differs between mouse and human cells in the requirement for STAT1. Virology. 2015;485:363-70. Epub 20150831. doi: 10.1016/j.virol.2015.08.001. PubMed PMID: 26335850; PMCID: PMC4619148.
41. Herbert A, Alfken J, Kim YG, Mian IS, Nishikura K, Rich A. A Z-DNA binding domain present in the human editing enzyme, double-stranded RNA adenosine deaminase. Proc Natl Acad Sci U S A. 1997;94(16):8421-6. doi: 10.1073/pnas.94.16.8421. PubMed PMID: 9237992; PMCID: PMC22942.
42. Roy ER, Wang B, Wan YW, Chiu G, Cole A, Yin Z, Propson NE, Xu Y, Jankowsky JL, Liu Z, Lee VM, Trojanowski JQ, Ginsberg SD, Butovsky O, Zheng H, Cao W. Type I interferon response drives neuroinflammation and synapse loss in Alzheimer disease. J Clin Invest. 2020;130(4):1912-30. doi: 10.1172/JCI133737. PubMed PMID: 31917687; PMCID: PMC7108898.
43. Sanford SAI, McEwan WA. Type-I Interferons in Alzheimer's Disease and Other Tauopathies. Front Cell Neurosci. 2022;16:949340. Epub 20220715. doi: 10.3389/fncel.2022.949340. PubMed PMID: 35910253; PMCID: PMC9334774.
44. Taylor JM, Minter MR, Newman AG, Zhang M, Adlard PA, Crack PJ. Type-1 interferon signaling mediates neuro-inflammatory events in models of Alzheimer's disease. Neurobiol Aging. 2014;35(5):1012-23. Epub 20131029. doi: 10.1016/j.neurobiolaging.2013.10.089. PubMed PMID: 24262201.
45. Bazak L, Levanon EY, Eisenberg E. Genome-wide analysis of Alu editability. Nucleic Acids Res. 2014;42(11):6876-84. doi: 10.1093/nar/gku414. PubMed PMID: 24829451; PMCID: PMC4066801.

Figure 1

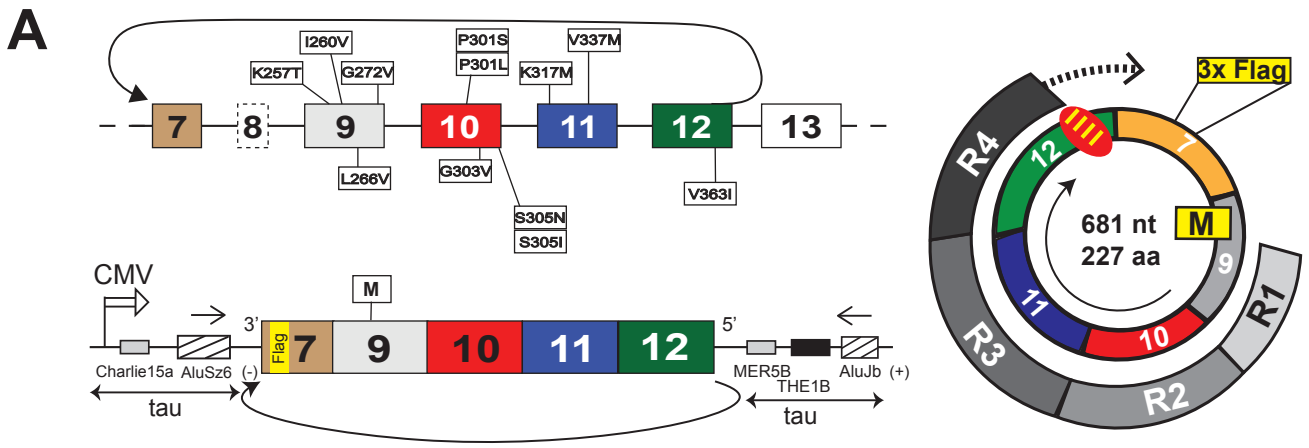
A
I260V
K257T
G272V
P301S
P301L
K317M
V337M
7
8
9
10
11
12
13
L266V
G303V
S305N
S305I
V363I
CMV
M
3'
5'
Flag
Charlie15a
AluSz6
(-)
MER5B
THE1B
AluJb
(+)
tau
tau
3x Flag
R4
R3
R2
R1
681 nt
227 aa
M

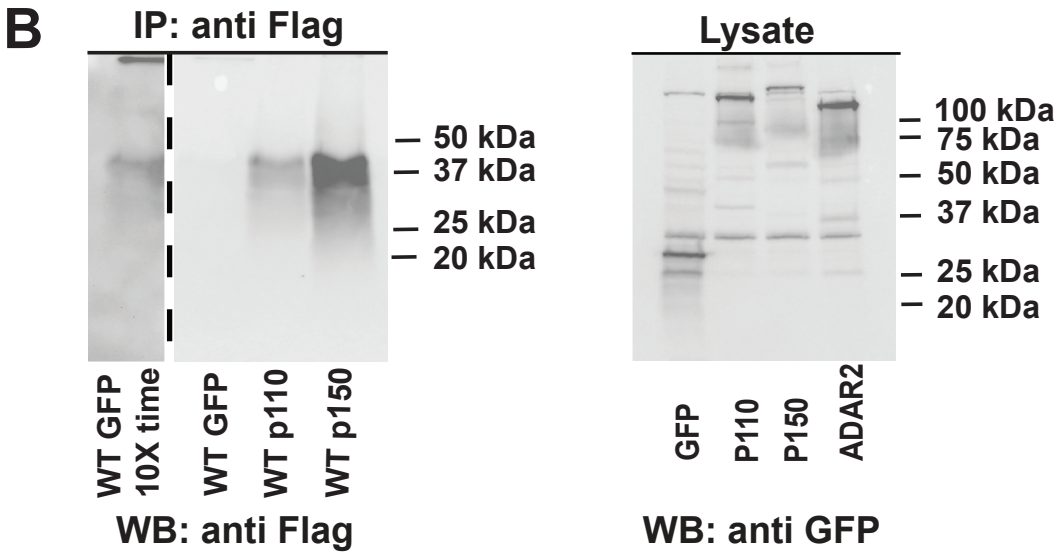
B
IP: anti Flag
50 kDa
37 kDa
25 kDa
20 kDa
WT GFP 10X time
WT GFP
WT p110
WT p150
WB: anti Flag
Lysate
100 kDa
75 kDa
50 kDa
37 kDa
25 kDa
20 kDa
GFP
P110
P150
ADAR2
WB: anti GFP

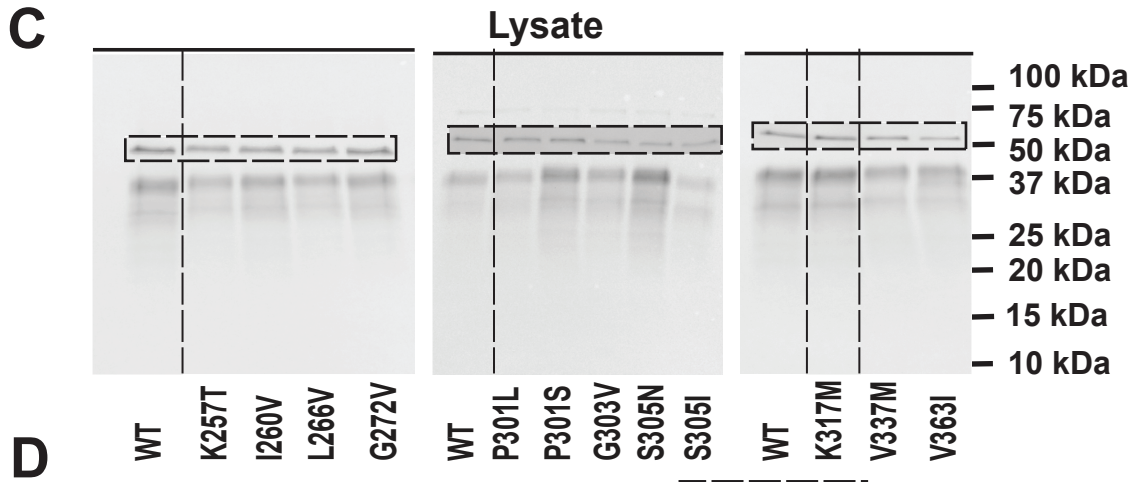
C
Lysate
100 kDa
75 kDa
50 kDa
37 kDa
25 kDa
20 kDa
15 kDa
10 kDa
WT
K257T
I260V
L266V
G272V
WT
P301L
P301S
G303V
S305N
S305I
WT
K317M
V337M
V363I

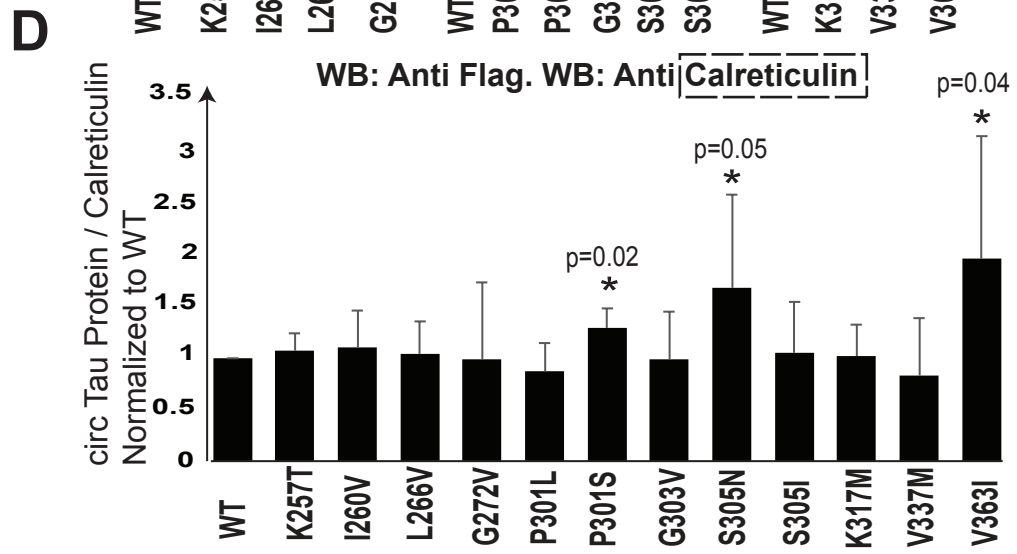
D
WB: Anti Flag. WB: Anti Calreticulin
circ Tau Protein / Calreticulin
Normalized to WT
3.5
3
2.5
2
1.5
1
0.5
0
p=0.02
*
p=0.05
*
p=0.04
*
WT
K257T
I260V
L266V
G272V
P301L
P301S
G303V
S305N
S305I
K317M
V337M
V363I

Figure 2

A

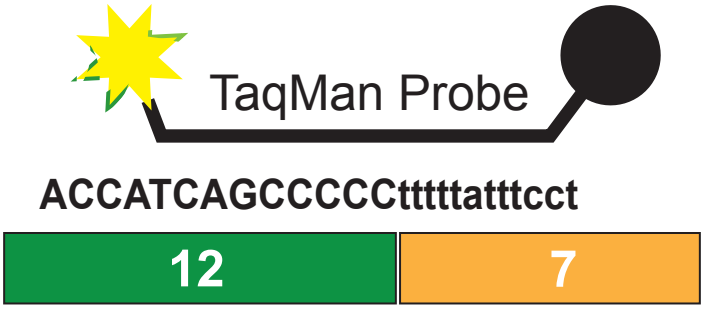
TaqMan Probe
ACCATCAGCCCCCtttttatttcct
12
7

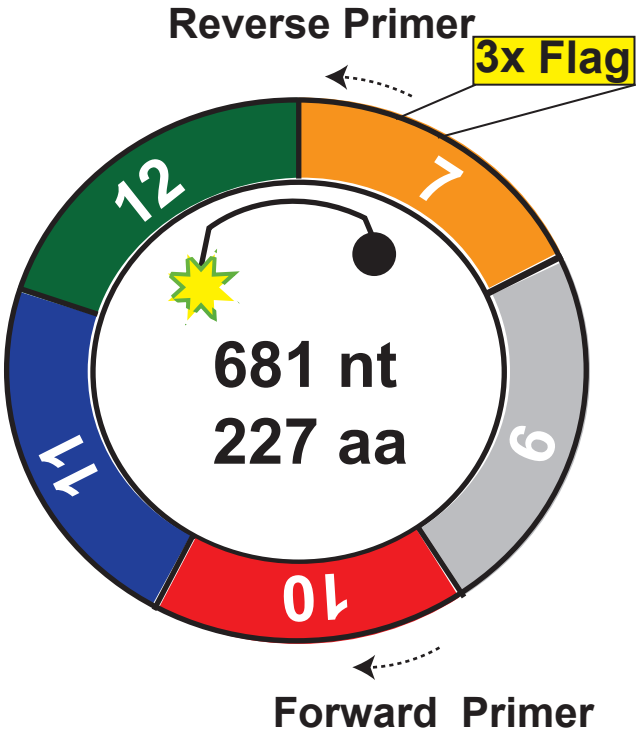
Reverse Primer
3x Flag
12
7
681 nt
227 aa
11
9
10
Forward Primer

B

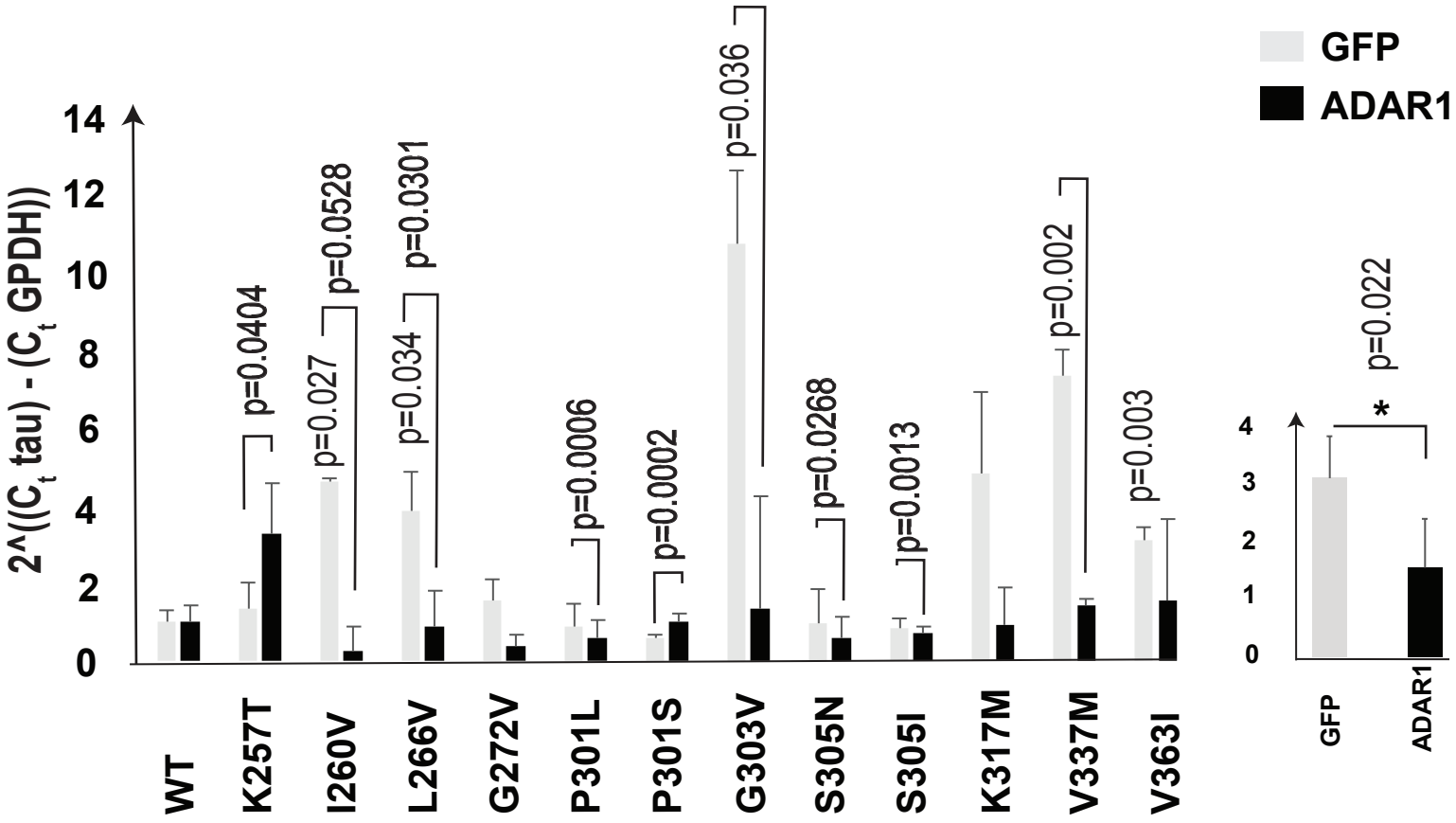
GFP
ADAR1
2^((C_t tau) - (C_t GPDH))
14
12
10
8
6
4
2
0
p=0.0404
p=0.027
p=0.0528
p=0.034
p=0.0301
p=0.0006
p=0.0002
p=0.036
p=0.0268
p=0.0013
p=0.002
p=0.003
WT
K257T
I260V
L266V
G272V
P301L
P301S
G303V
S305N
S305I
K317M
V337M
V363I
p=0.022
*
4
3
2
1
0
GFP
ADAR1

Figure 3

A

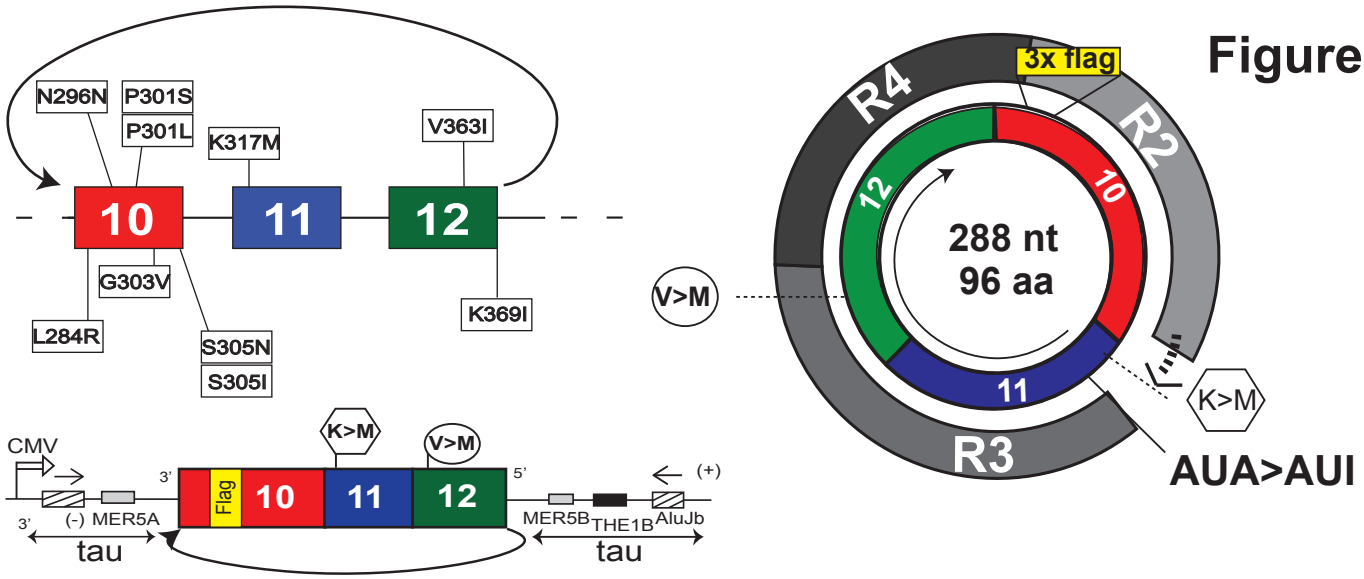

B

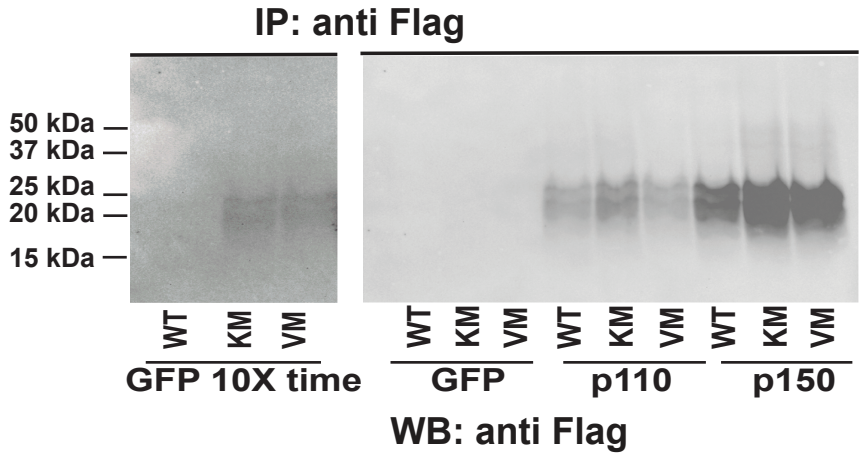

C

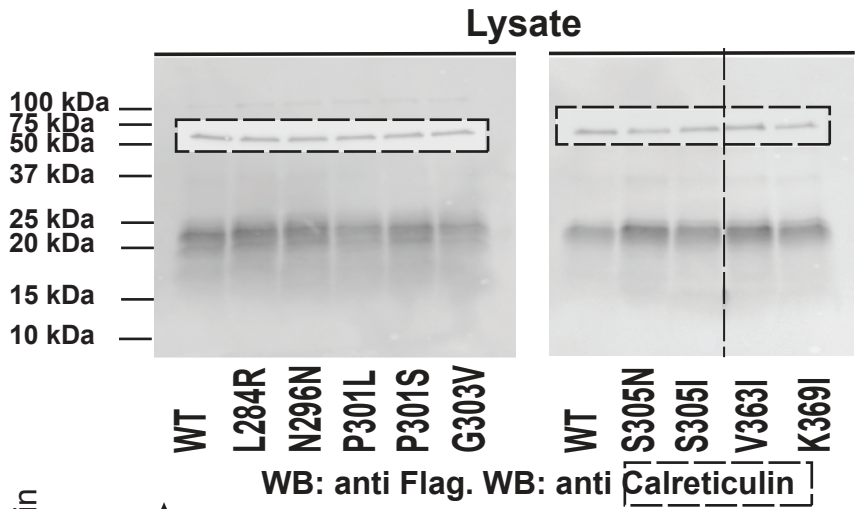

D

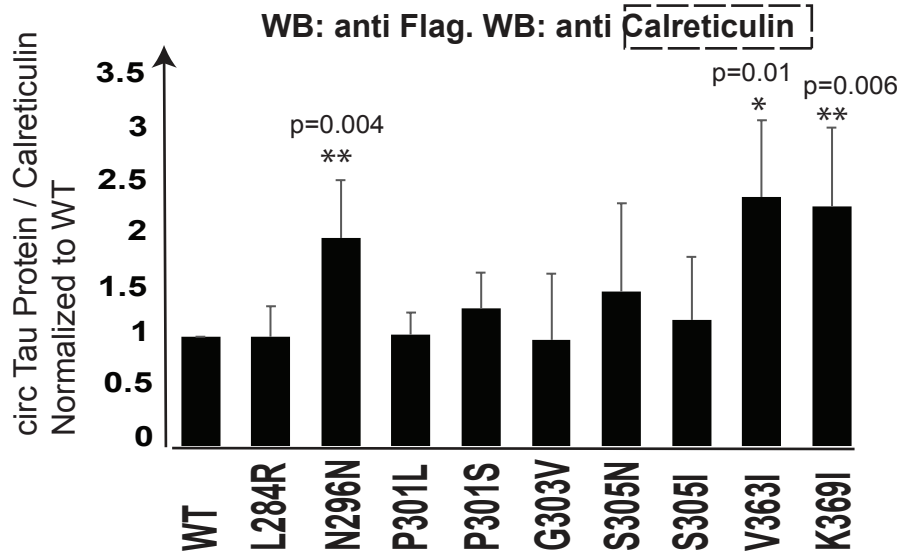

Figure 4

A

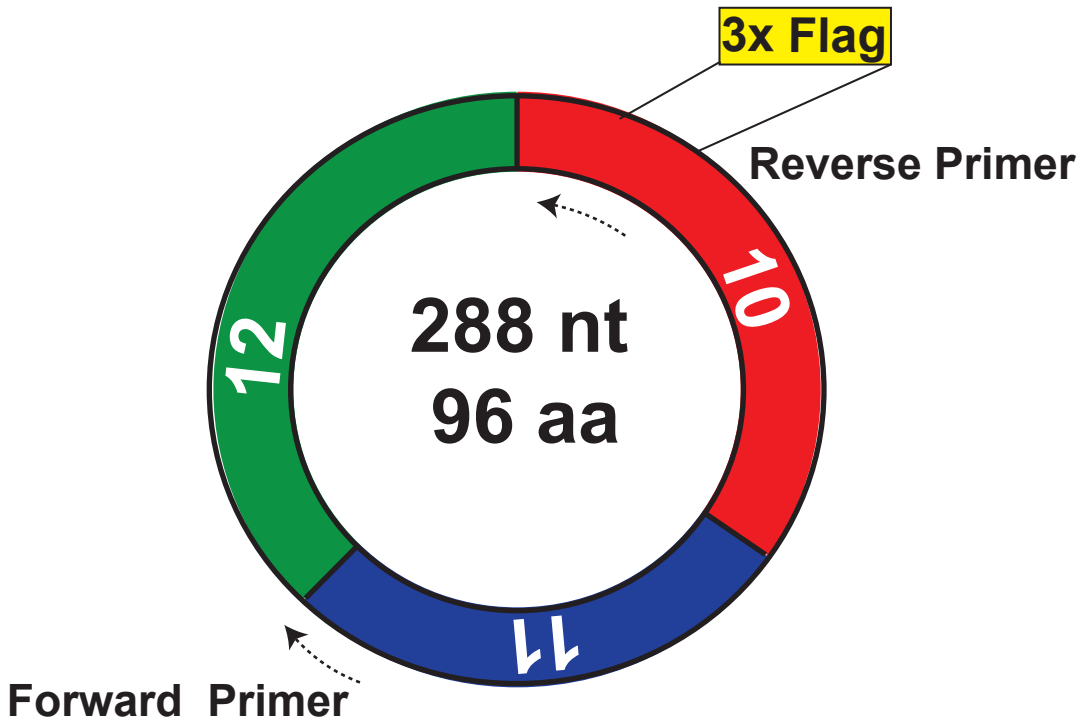
3x Flag
Reverse Primer
10
12
11
288 nt
96 aa
Forward Primer

B

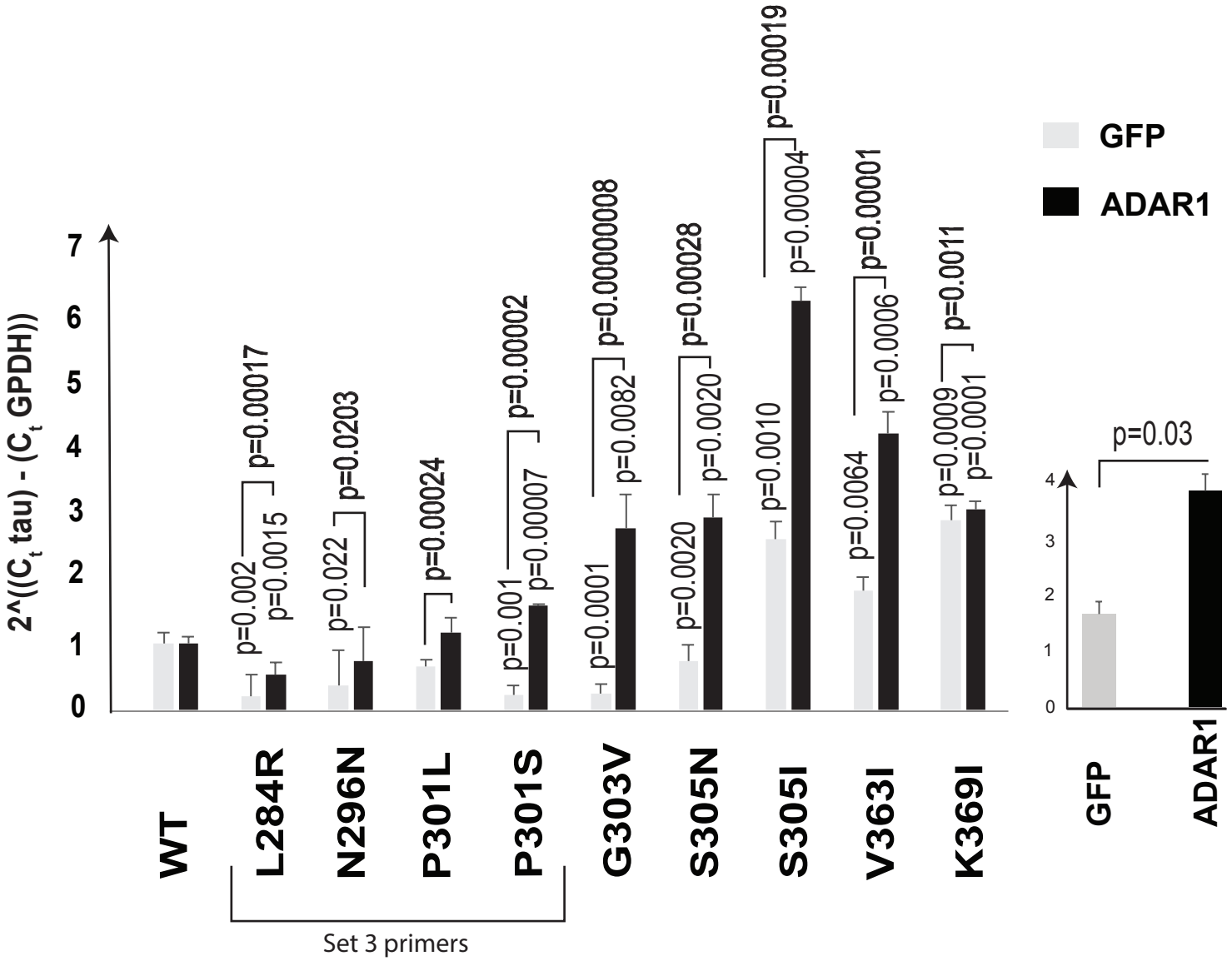
GFP
ADAR1
2^((C_t tau) - (C_t GPDH))
0
1
2
3
4
5
6
7
p=0.002
p=0.0015
p=0.00017
p=0.022
p=0.0203
p=0.00024
p=0.001
p=0.00007
p=0.00002
p=0.0001
p=0.0082
p=0.00000008
p=0.0020
p=0.0020
p=0.00028
p=0.0010
p=0.00004
p=0.00019
p=0.0064
p=0.0006
p=0.00001
p=0.0009
p=0.0001
p=0.0011
WT
L284R
N296N
P301L
P301S
G303V
S305N
S305I
V363I
K369I
Set 3 primers
p=0.03
GFP
ADAR1

Figure 5

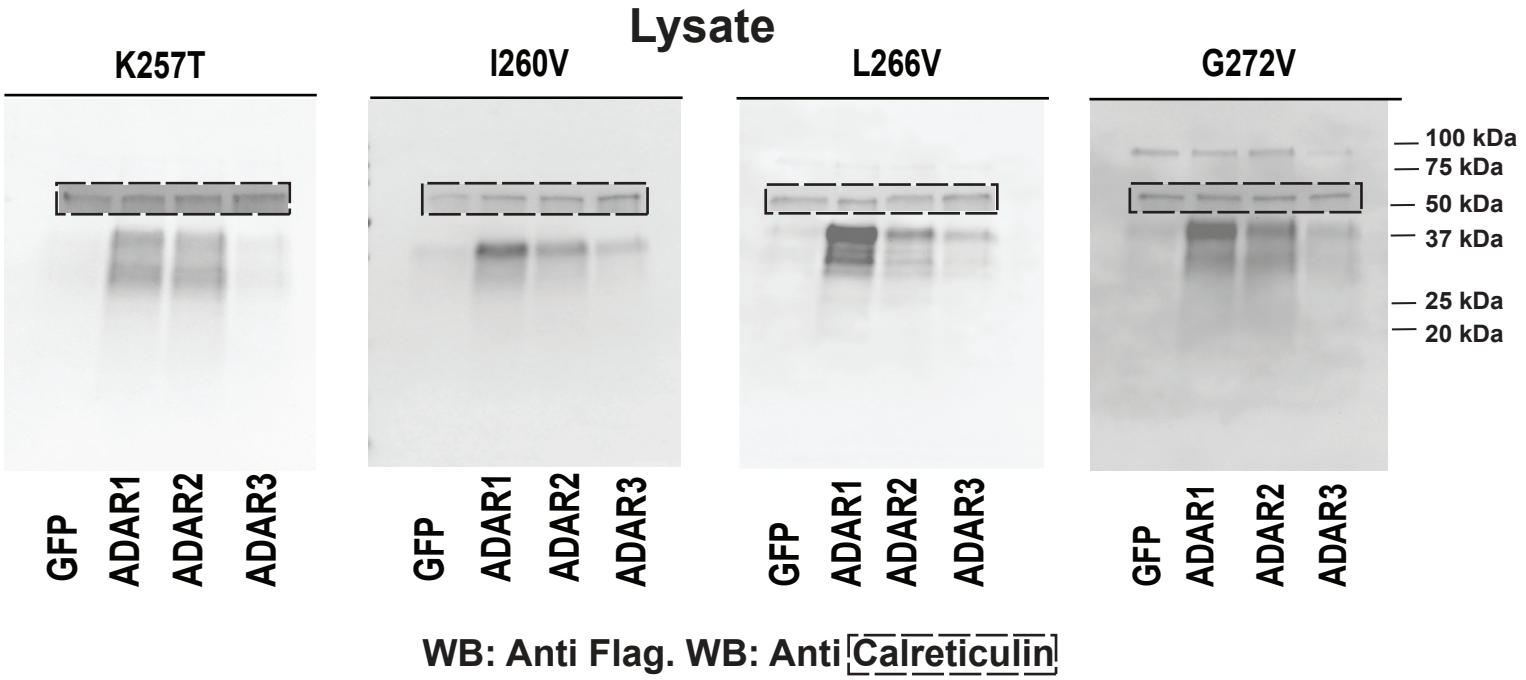
Lysate
K257T
I260V
L266V
G272V
100 kDa
75 kDa
50 kDa
37 kDa
25 kDa
20 kDa
GFP
ADAR1
ADAR2
ADAR3
WB: Anti Flag. WB: Anti Calreticulin

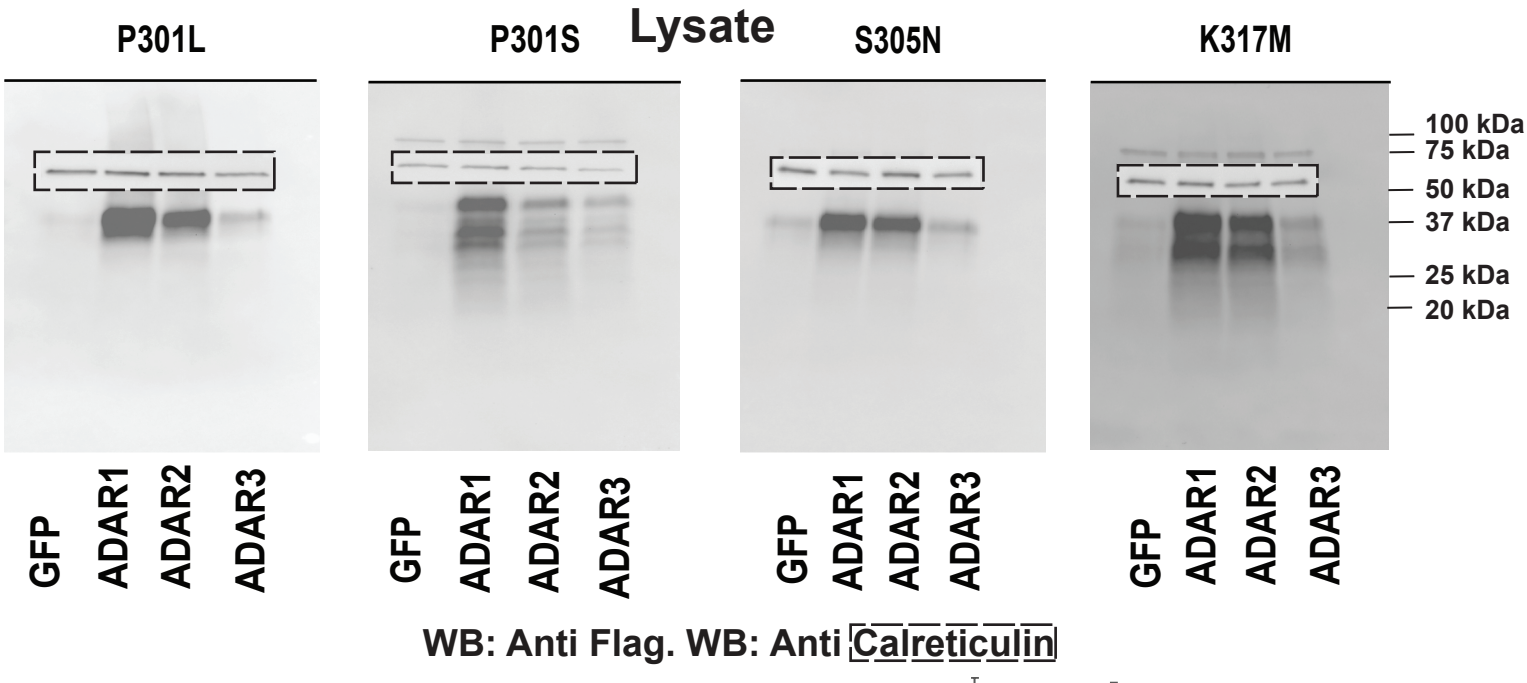
Lysate
P301L
P301S
S305N
K317M
100 kDa
75 kDa
50 kDa
37 kDa
25 kDa
20 kDa
GFP
ADAR1
ADAR2
ADAR3
WB: Anti Flag. WB: Anti Calreticulin

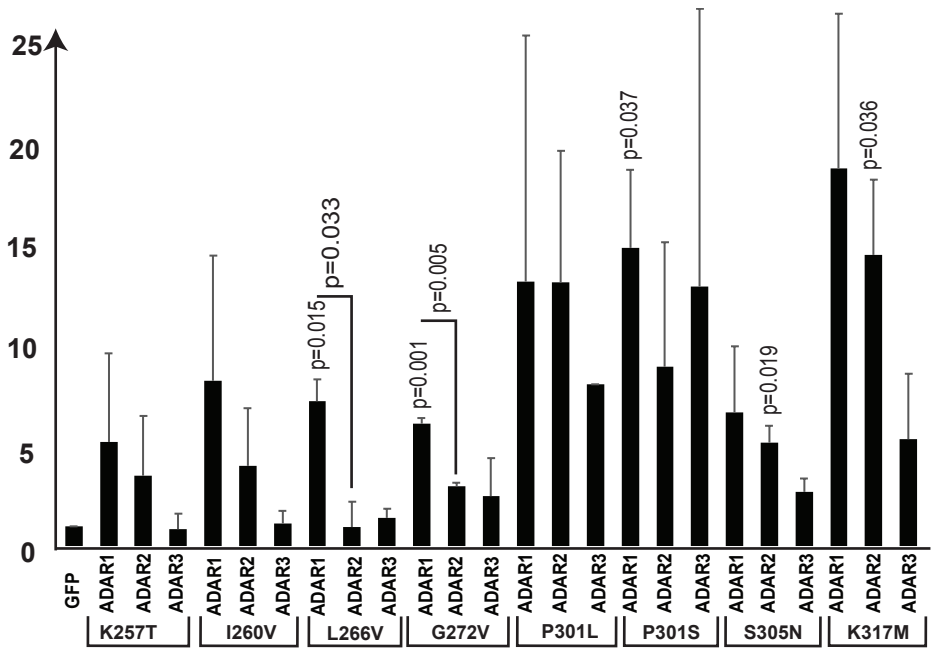
25
20
15
10
5
0
p=0.015
p=0.033
p=0.001
p=0.005
p=0.037
p=0.019
p=0.036
GFP
ADAR1
ADAR2
ADAR3
K257T
I260V
L266V
G272V
P301L
P301S
S305N
K317M

Figure 6

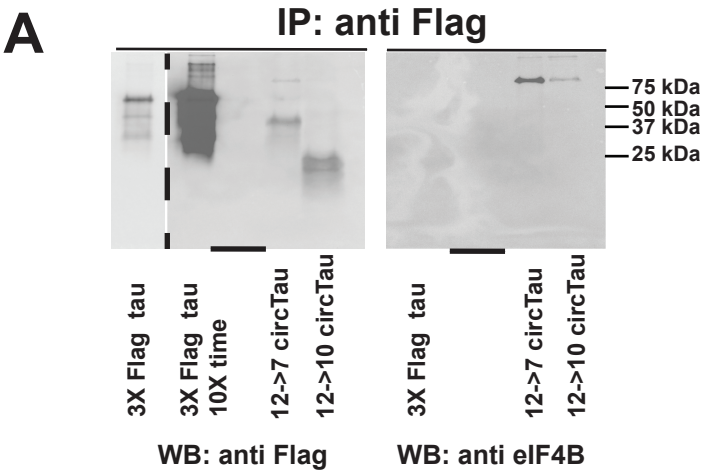
A
IP: anti Flag
75 kDa
50 kDa
37 kDa
25 kDa
3X Flag tau
3X Flag tau 10X time
12->7 circTau
12->10 circTau
3X Flag tau
12->7 circTau
12->10 circTau
WB: anti Flag
WB: anti eIF4B

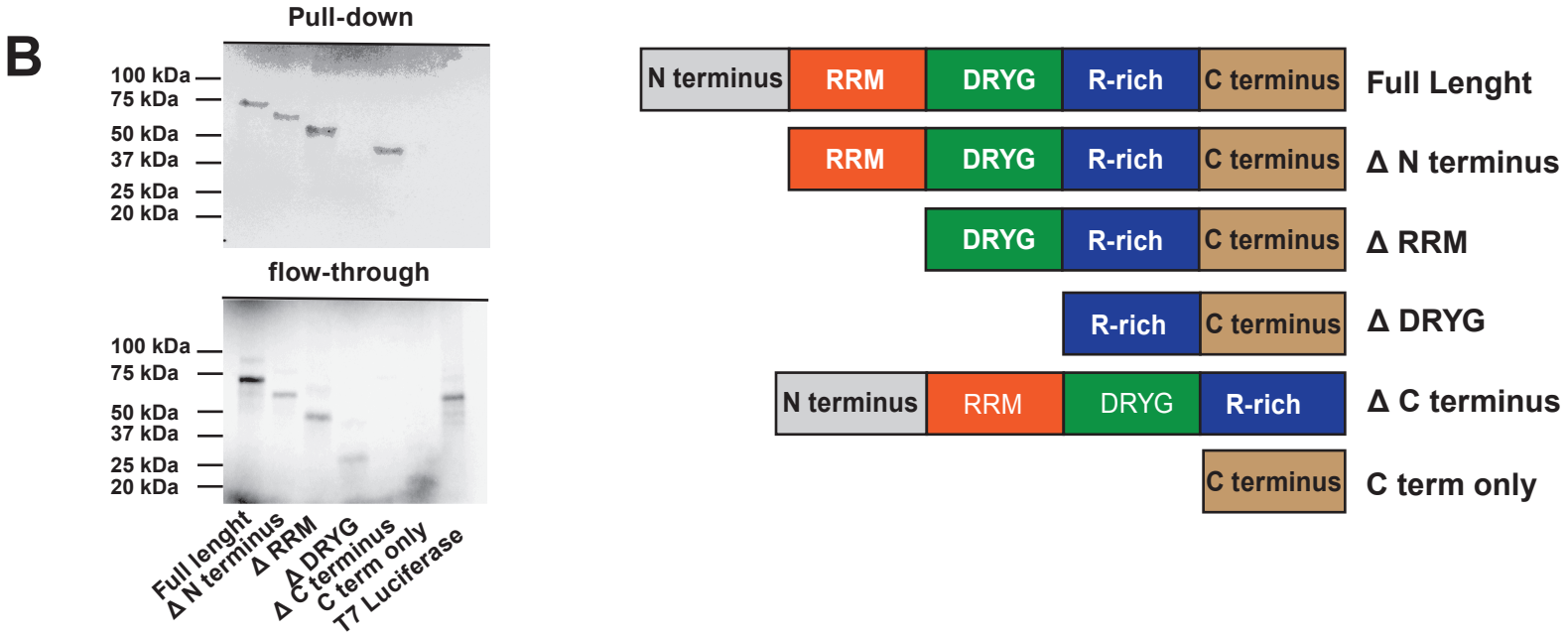
B
Pull-down
100 kDa
75 kDa
50 kDa
37 kDa
25 kDa
20 kDa
flow-through
100 kDa
75 kDa
50 kDa
37 kDa
25 kDa
20 kDa
Full lenght
Δ N terminus
Δ RRM
Δ DRYG
Δ C terminus
C term only
T7 Luciferase
N terminus
RRM
DRYG
R-rich
C terminus
Full Lenght
Δ N terminus
Δ RRM
Δ DRYG
Δ C terminus
C term only

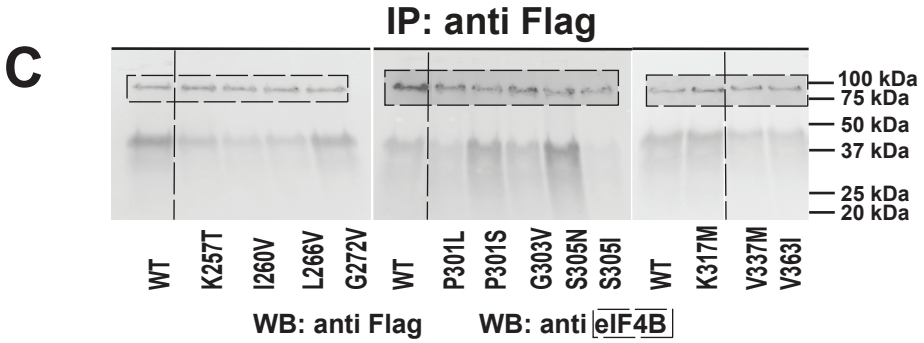
C
IP: anti Flag
100 kDa
75 kDa
50 kDa
37 kDa
25 kDa
20 kDa
WT
K257T
I260V
L266V
G272V
WT
P301L
P301S
G303V
S305N
S305I
WT
K317M
V337M
V363I
WB: anti Flag
WB: anti eIF4B

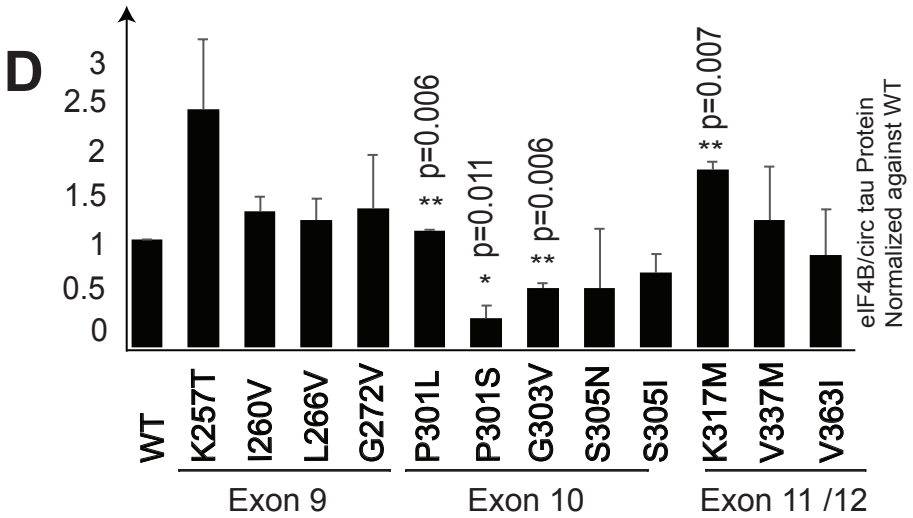
D
3
2.5
2
1.5
1
0.5
0
** p=0.006
* p=0.011
** p=0.006
** p=0.007
eIF4B/circ tau Protein
Normalized against WT
WT
K257T
I260V
L266V
G272V
P301L
P301S
G303V
S305N
S305I
K317M
V337M
V363I
Exon 9
Exon 10
Exon 11 /12

Figure 7

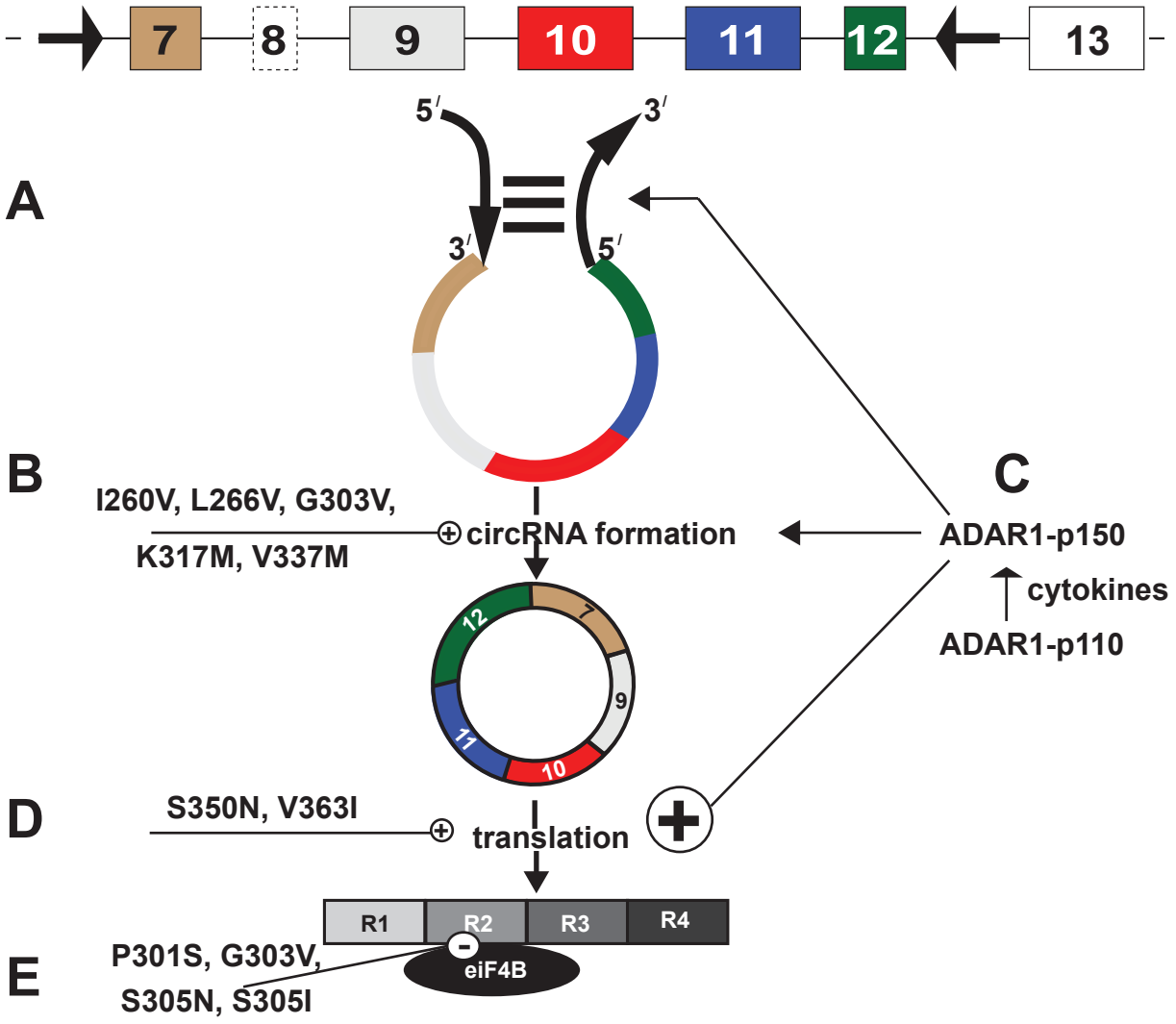
7
8
9
10
11
12
13
A
5′
3′
3′
5′
B
I260V, L266V, G303V,
K317M, V337M
circRNA formation
C
ADAR1-p150
cytokines
ADAR1-p110
12
7
9
11
10
D
S350N, V363I
translation
R1
R2
R3
R4
eiF4B
E
P301S, G303V,
S305N, S305I